arXiv:cond-mat/0109387v1 [cond-mat.str-el] 21 Sep 2001

New aspects of Verway transition in magnetite

Hitoshi Seo[1], Masao Ogata[2], and Hidetoshi Fukuyama[3]
[1] *Correlated Electron Research Center (CERC),*
National Institute of Advanced Industrial Science and Technology, Ibaraki 305-8562, Japan
[2] *Department of Physics, University of Tokyo, Tokyo 113-0033, Japan*
[3] *Institute for Solid State Physics, University of Tokyo, Chiba 277-8581, Japan*
(February 1, 2008)

Abstract

A new mechanism of the Verway transition in magnetite (Fe_3O_4), which has been argued to be a charge ordering transition so far, is proposed. Based on the mean field calculations for the three band model of spinless fermions appropriate for the d electrons of the Fe ions on the B sites, it is indicated that the phase transition should be the bond dimerization due to the cooperative effects of strong electronic correlation and electron-phonon interaction. The results show that the ferro-orbital ordered state is stabilized in a wide temperature range due to the strong on-site Coulomb interaction between different t_{2g} orbitals resulting in an effectively one-dimensional electronic state, which leads the system toward an insulating state by the Peierls lattice distortion with the period of two Fe(B) ions, i.e., bond dimerization. Furthermore, it is found that the interplay between such lattice distortion in the Fe(B) ions and the lattice elastic energy of the Fe(B)-O as well as the Fe(A)-O bonds gives rise to a competition between two different three-dimensional patterns for the bond dimerization, and can stabilize a complicated one with a large unit cell size. The results are compared with the known experimental facts.

PACS: 71.10.Fd,71.30.+h,71.10.Hf,75.50.Gg

I. INTRODUCTION

The nature of the Verway transition in magnetite (Fe_3O_4) has not been clarified yet, in spite of intensive studies from very early days [1]. Fe_3O_4 forms the cubic spinel structure, as shown in Fig. 1, where one-third of the Fe ions occupy the A sites, tetrahedrally coordinated by 4 oxygen ions, while the remaining two-third are octahedrally surrounded by 6 oxygen ions, which are the B sites. One can see that Fe$(B)_2O_4$ layers and Fe(A) layers are stacked alternatively, while the z axis can be taken as any of the three cubic crystal axes. Although the primitive cell is a rhombohedral parallelepiped containing 2 formula units of Fe_3O_4, the unit cell is conveniently chosen as the cubic one, as shown in Fig. 1, containing 8 formula units, to which we also refer in this paper.

The Fe(A) ions are trivalent while the Fe(B) ions are mixed valent with formal average valence Fe$(B)^{2.5+}$. Below $T_{\rm N} = 858$ K, the magnetic moments of the Fe ions are ferrimagnetically ordered, where the A sites and the B sites have opposite spin directions, with d-orbital occupation represented as $(t_{2g\uparrow})^3(e_{g\uparrow})^2$ and $(t_{2g\downarrow})^3(e_{g\downarrow})^2(t_{2g\uparrow})^{0.5}$, respectively. Well below $T_{\rm N}$, an abrupt increase in the resistivity takes place at $T_{\rm V} \simeq 120$ K, which is now called after Verway, who has discovered it [2] and proposed that the phenomena is due to the ordering of equal number of Fe^{2+} and Fe^{3+} on the B sites, i.e., charge ordering (CO) among the "extra" $t_{2g\uparrow}$ electrons [3].

As for theoretical studies on this phenomena, the electronic properties of the spin polarized $t_{2g\uparrow}$ electrons have been investigated frequently by the single band spinless fermion model on the B sites originally proposed by Cullen and Callen [4,5]. Such a picture of spinless fermion has been proved to be valid by band structure calculations [6–8], where the majority spin ($\downarrow$) band of the Fe(B) ions is shown to be fully occupied and the Fermi energy crosses the minority spin ($\uparrow$) band. In the model of Cullen and Callen the triple degeneracy of the t_{2g} orbitals is neglected so that the band is half-filled, corresponding to half a charge per site as in the actual compound. This model is investigated within the Hartree approximation where the ground state shows a phase transition from a metallic state to a CO state as the intersite Coulomb interaction V_{ij} is increased [4], providing the most naive picture for the CO state in the magnetite.

However, no CO pattern so far considered has been successful in presenting a satisfactory interpretation for the known experiments, including the one originally proposed by Verway [3] and other more complicated patterns [9,10]. Besides, the expected short range fluctuation of the CO due to the frustration in V_{ij} [11], arising from the fact that the network connecting the Fe(B) ions forms a coupled tetrahedra system, is not found either in neutron scattering [12] or in resonant X-ray scattering measurements [13]. Furthermore, the recent NMR [14] and X-ray anomalous scattering [15] experiments for $T < T_{\rm V}$ even cast doubts on the existence of CO. Todo *et al.* [16], based on these suggestions and their finding of pressure-induced metallic ground state above 8 GPa, proposed that the low temperature phase below $T_{\rm V}$ may be a kind of "Mott insulator" where the B sites are forming dimers due to orbital ordering (OO).

This idea of the Mott insulating state resembles to that in low-dimensional quarter-filled organic conductors theoretically studied by Kino and the present authors [17], where the fact that there exists a carrier per 2 sites is the same as that for the B sites in Fe_3O_4. In such organic conductors, the Mott insulating state can be understood from a view point

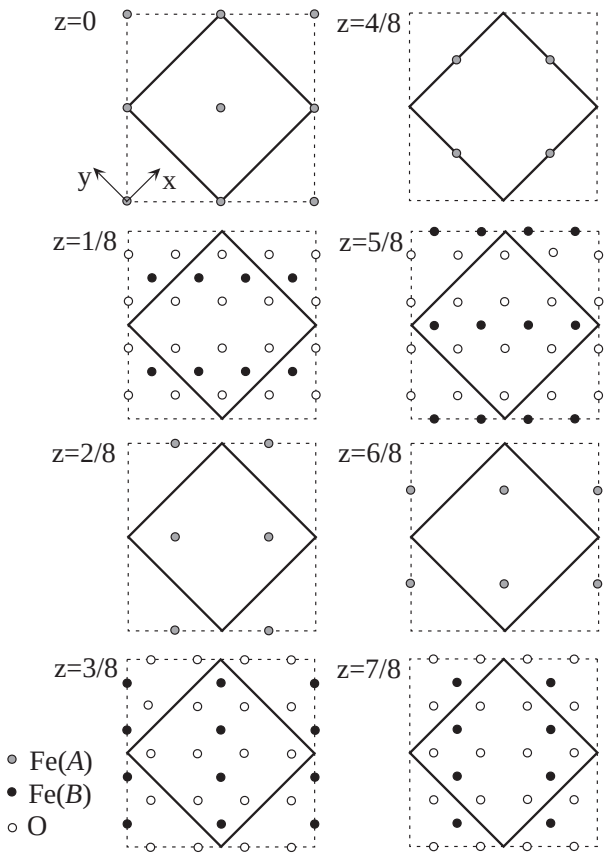

FIG. 1. Cubic spinel structure of Fe_3O_4. The thick square shows the cubic unit cell with a lattice constant a in the xy plane while the z coordinates are indicated by the fraction of a. The unit cell in the xy plane for $T < T_V$ is shown by the dotted line.

that each charge localizes in every two sites, i.e., dimer. The dimerization is either due to the anisotropy in the transfer integrals from the lattice structure [18], or due to the spontaneous formation of bond dimerization (BD) by the electron-phonon interaction where the one-dimensionality (1D) plays a crucial role [19].

In this paper, we will show that this latter type of insulating state with BD can actually emerge in Fe_3O_4, and propose it to be the mechanism of the Verway transition in this compound. We will discuss in Sec. II that the strong correlation among electrons stabilizes an OO state with effectively 1D electronic structure, and additional electron-phonon interaction can give rise to the BD state. Moreover, discussions in Sec. III on the elastic lattice energy of the whole system will lead to the three-dimensional pattern of this BD expected below T_V. The relevance of our proposal to the experimental facts is discussed in Sec. IV, and the conclusion is given in Sec. V.

II. BOND DIMERIZATION ON B SITES

A. Three band model

We start with the model of Mishra *et al.* [20], who have extended the spinless fermion model of Cullen and Callen [4] by including the triple degeneracy of the t_{2g} orbitals appropriate for the B sites in Fe_3O_4. The Hamiltonian is written as

$$H = \sum_{\langle ij \rangle} \sum_{\mu\nu} t_{ij}^{\mu\nu} c_{i\mu}^{\dagger} c_{j\nu} + \sum_{i} \sum_{\mu \neq \nu} U n_{i\mu} n_{i\nu} + \sum_{\langle ij \rangle} V n_i n_j, \tag{1}$$

where $c_{i\mu}^{\dagger}$ ($c_{i\mu}$) and $n_{i\mu}$ denote the creation (annihilation) and the number operator of the electron at ith site of orbital μ, respectively, where the orbital indices take xy, yz or zx [21]. n_i is the number operator for each site, i.e., $n_i = n_{ixy} + n_{iyz} + n_{izx}$, and $\langle ij \rangle$ denotes the nearest-neighbor site pair along the coupled Fe(B) ion tetrahedra network. U and V are the on-site Coulomb energy between different orbitals (note that the same orbital cannot be doubly occupied) and the nearest-neighbor Coulomb energy, respectively. By using the transfer integrals for $\langle ij \rangle$ pairs calculated in Ref. 7, $t_{dd\sigma} = -0.41$ eV, $t_{dd\pi} = 0.054$ eV and $t_{dd\delta} = 0.122$ eV, the three kinds of transfer integrals, $t_{ij}^{\mu\nu}$, with different configurations of orbital occupations, as shown in Fig. 2, can be estimated [22] as $t_1 = 3t_{dd\sigma}/4 + t_{dd\delta}/4 = -0.278$ eV, $t_2 = t_{dd\pi}/2 + t_{dd\delta}/2 = 0.085$ eV and $t_3 = t_{dd\sigma}/2 - t_{dd\delta}/2 = -0.035$ eV, where the notations of $t_{1\sim3}$ are given in Fig. 2.

Mishra *et al.* treated the Coulomb interaction terms, U and V, by means of Hartree mean field approximation,

$$n_{i\mu} n_{j\nu} \rightarrow \langle n_{i\mu} \rangle n_{j\nu} + n_{i\mu} \langle n_{j\nu} \rangle - \langle n_{i\mu} \rangle \langle n_{j\nu} \rangle , \tag{2}$$

and determined the ground state of the system. Their results for the case with the fixed value of $U = 4.0$ eV, relevant for magnetite [7], showed that the CO state is stabilized in the ground state for $V > V_c = 0.38$ eV [23] while the metallic state is for $V < V_c$, qualitatively the same as in the one-band model [4], and they concluded that the former state is relevant for the magnetite.

Although it is not emphasized in their paper, every site is almost fully occupied by the same orbital state, namely, ferro-OO is realized in both of these states, due to the large

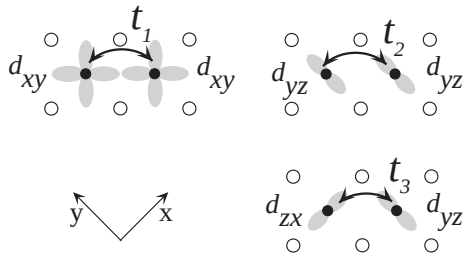

FIG. 2. A schematic representation of the transfer integrals between neighboring B site pairs in the xy plane with different orbital occupations. The simultaneous cyclic substitution of the orbital indices and the axes of coordinates, $x \rightarrow y, y \rightarrow z, z \rightarrow x$ or $x \rightarrow z, y \rightarrow x, z \rightarrow y$, also provides the three transfer integrals, while for the other configurations $t_{ij}^{\mu\nu}$=0.

value of U. The three d_{xy}-, d_{yx}- and d_{yz}-OO states are energetically degenerate, and the electronic structure becomes 1D once one of the OO state is realized, which is particular to the spinel structure. For example the d_{xy}-OO state has 1D arrays of sites connected by the largest transfer integral t_1, which are along the [110] direction and the [1$\bar{1}$0] direction for the xy planes with z coordinates $z = (4n+1)/8$ and $z = (4n+3)/8$, respectively (see Fig. 1).

In the metallic state with the presence of this d_{xy}-OO, the expectation values of the charge density for all sites are $\langle n_{ixy} \rangle \simeq 0.5$ and $\langle n_{iyz} \rangle = \langle n_{izx} \rangle \simeq 0$. As for the CO state, i.e., the coexistent state of OO and CO, the planes with 1D arrays of $\langle n_{ixy} \rangle \simeq 0.5 + \delta$ and those with $\langle n_{ixy} \rangle \simeq 0.5 - \delta$, corresponding to Fe^{2+} and Fe^{3+}, respectively, are stacked alternatively along the z direction, where the CO pattern is the one proposed by Verway. Here δ is the amount of charge disproportionation, which rapidly increases as the value of V is increased from V_c, and reaches around 0.9 for $V = 1.0$ eV. The other two d_{yz} and d_{zx} orbitals are almost empty also in the CO state.

In contrast to their conclusion that this CO state is realized in magnetite, the recent experimental proposals of the absence of CO mentioned in Sec. I suggest that the former *OO metallic* state should be relevant to the actual system, and that the origin of insulator is other than CO. The destabilization of the CO state may be due to the screening of the long range Coulomb interaction and/or the effect of frustration among V_{ij} mentioned above [11]. Actually, the melting of CO due to frustration among V_{ij} has been demonstrated theoretically in 1D systems [24], though we will not discuss such possibility in magnetite further in this paper. Here we will concentrate in the following on how the OO metallic state shows instability toward an insulating state and its possible consequence on the lattice structure in this insulating phase.

B. Peierls instability in orbital ordered state

In the following we consider the case of the d_{xy}-OO metallic state. The properties of this ferro-OO state can be extracted by an effective noninteracting 1D spinless fermion system, $H_{1D} = \sum_l t_1 (c_l^\dagger c_{l+1} + h.c.)$, with a half-filled band, l being the site index along the 1D directions [110] or [1$\bar{1}$0]. This model should be valid for $U \gg t_1 \gg t_2, t_3$ in eq. (1) with $V_{ij} = 0$. It is well known that such a half-filled 1D band has the Peierls instability with the wavelength of two times the inter-atomic distance [19], i.e., *instability toward the BD state* with alternating atomic displacements along the 1D direction. Actually the system can be mapped onto the $S = 1/2$ XY chain via Jordan-Wigner transformation, so that our metallic state here correspond to the spin liquid state, which shows instability toward the spin-Peierls state, that is, the BD state in spin system. Thus, once the electron-phonon interaction is present, the OO state in magnetite will undergo a BD transition to gain kinetic energy by making a gap at the band center, resulting in an *insulating* state. We propose this scenario to be the origin of the insulating ground state of magnetite, Fe_3O_4. Such a state will be realized if it is not destroyed by the inter-chain interactions t_2 and t_3, which is investigated in the next subsection.

We should note that this Peierls instability is different from the usual one in the 1D electron system of weak coupling, since the assumption of the spinless fermion here is due to the ferrimagnetic spin ordering realized in the limit of infinite value of on-site intra-orbital

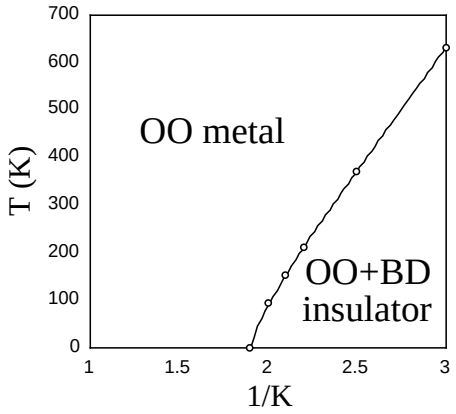

FIG. 3. Mean field phase diagram for the three-band Peierls-Hubbard model for the B sites, on the plane of temperature, T, and the inverse of the lattice elastic coupling constant, $1/K$. OO and BD represent orbital-ordering and bond dimerization, respectively.

Coulomb interaction. Thus one may say that the BD state here is rather analogous to the Mott insulator in quarter-filled compounds noted in Sec. I [17–19], where the origin is also the interplay between the strong on-site Coulomb interaction and the dimerization.

C. Peierls-Hubbard model

To investigate the stability of the BD state in the actual three-dimensional system, we include the lattice degree of freedom by adding the Peierls-type coupling to Eq. (1), i.e., treat the Peierls-Hubbard model for magnetite. It is expressed as

$$H_{\rm PH} = \sum_{<ij>}\sum_{\mu\nu} t_{ij}^{\mu\nu}(1+u_{ij})c_{i\mu}^{\dagger}c_{j\nu} + \sum_{i}\sum_{\mu\neq\nu} U n_{i\mu}n_{i\nu} + \sum_{i}\frac{1}{2}Ku_{ij}^{2}, \tag{3}$$

where u_{ij} and K are the lattice distortion between nearest-neighbor site pair $\langle ij\rangle$ and the coupling constant for the elastic energy, respectively. The intersite Coulomb interaction term is neglected here since it is not relevant in our discussion as mentioned in Sec. II A. The on-site Coulomb interaction term, U, is treated within the mean field approximation, as in eq. (2), and self-consistent solutions are obtained. We restrict ourselves to the case of $u_{ij} = (-1)^l u$ associated with the three kinds of transfer integrals along the [110] and $[1\bar{1}0]$ directions and $u_{ij} = 0$ for the other directions. This provides the BD state, u being the degree of BD, and the value of u is determined for each choice of parameters so as to minimize the energy. We note that the calculated energy does not depend on different BD patterns since the effect of the lattice distortion on the lattice elastic energy and on the transfer integrals is restricted in each chains.

The results show that the BD state can actually be stabilized when $1/K$ exceeds a critical value. In Fig. 3, the obtained phase diagram within the finite temperature mean field approximation is shown for the case of fixed $U = 4.0$ eV, the same as in the calculation of Mishra *et al.* [20] mentioned in Sec. II A. The ground state is OO metallic with $u = 0$

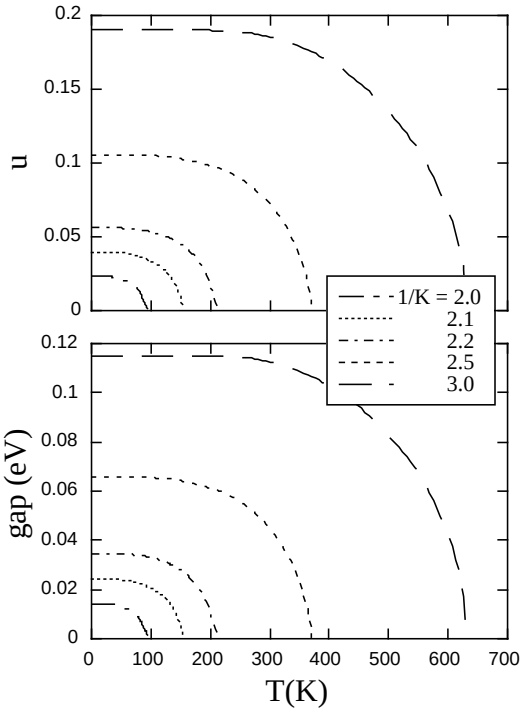

FIG. 4. Temperature dependences of (a) the degree of BD, u, and (b) the band gap for several values of $1/K$.

below $1/K < 1.9$ eV^{-1}, whereas the OO state with $u \neq 0$, i.e., the BD state, is stabilized for $1/K > 1.9$ eV^{-1}, where the system is insulating. Below $T_{\rm OO} \simeq 6000$ K, which is the temperature range shown in Fig. 3, the ferro-OO is present, and the para-orbital state is stabilized only above $T_{\rm OO}$.

The optimized value of u and the band gap in the BD state are plotted as a function of T in Figs. 4(a) and 4(b), respectively. It can be seen that the lattice dimerization and the band gap decrease as the temperature is increased and vanish continuously at $T = T_{\rm c}$, showing a second order insulator-to-metal phase transition. On the other hand, the charge density for each orbital state does not change noticeably from $\langle n_{ixy} \rangle \simeq 0.5$ and $\langle n_{iyz} \rangle = \langle n_{izx} \rangle \simeq 0$, for all sites, in the temperature range we are concerned. In other words, the OO is not affected through the metal-insulator transition.

III. BOND DIMERIZATION PATTERN

The three-dimensional BD pattern in the actual compound cannot be determined by the preceding calculation alone, since the calculated energy does not depend on the inter-chain configuration, as mentioned above. To discuss theoretically the stability of different BD states, the lattice elastic energy should be the most important factor since the BD produces large lattice distortion so that it moderately affects the lattice energy. The influence of the BD on the the inter-chain transfer integrals would be small so the difference in the kinetic energy between different BD states is neglected in the following discussion.

The lattice elastic energy in Fe_3O_4, $\mathcal{E}_{\rm lat}$, can be estimated by the sum of $\frac{K}{2}(\Delta u)^2$ for all the nearest neighbor Fe-O bonds, where Δu is the deviation of the Fe-O distance from that

in the equilibrium position above $T_{\rm V}$ and K is the elastic constant. The value of K should take common values $K_{\rm A}$ for the Fe(A)-O bonds and $K_{\rm B}$ for the Fe(B)-O bonds, since all the Fe(A)-O bonds as well as the Fe(B)-O bonds are respectively crystallographically equivalent above $T_{\rm V}$. Thus $\mathcal{E}_{\rm lat}$ can be expressed as $\mathcal{E}_{\rm Alat} + \mathcal{E}_{\rm Blat}$, for the Fe($A$)-O and the Fe($B$)-O bonds, respectively, where

$$\mathcal{E}_{\rm Alat} = \sum \frac{K_{\rm A}}{2}(\Delta u_{\rm A-O})^2, \tag{4}$$

$$\mathcal{E}_{\rm Blat} = \sum \frac{K_{\rm B}}{2}(\Delta u_{\rm B-O})^2, \tag{5}$$

where $\Delta u_{\rm A-O}$ and $\Delta u_{\rm B-O}$ are Δu for the Fe(A)-O and Fe(B)-O bonds, respectively.

Then, as will be explained in detail later, there are two candidates for the BD states costing much less elastic energy than the others, as schematically shown in Fig. 5(a) and (b). In the former the dimerization pattern between adjacent 1D chains in the xy plane is in-phase, thus we call it the in-phase BD state, where the unit cell is unchanged from the cubic unit cell above $T_{\rm V}$. On the other hand, in the latter pattern the BD is anti-phase, which is called anti-phase BD state in the following. Here, the unit cell becomes large as $\sqrt{2}\times\sqrt{2}\times 2$ of the cubic one, as shown in the Figure. We will see below that the competition between two BD states arises depending on the relative value of $K_{\rm A}$ and $K_{\rm B}$, and our proposal is that the anti-phase BD pattern is realized in the actual compound.

To see this competition, let us calculate a semi-phenomenological Landau-type free energy by taking into account of both in-phase and anti-phase BD states. We consider the amount of lattice distortion for the BD in the Fe(B) ions to be uniform along each chains, denoted by u_1 and u_2, for alternative chains in the xy planes. Then the in-phase BD is characterized by $u_1 = u_2$ while the anti-phase BD is by $u_1 = -u_2$, as shown in Fig. 6(a) and (b), respectively. The motions of oxygens are approximated to be perpendicular to the chains in the xy planes, parametrized by $u_{\rm O1}$ and $u_{\rm O2}$, for the chains with BD of u_1 and u_2, respectively. Within these approximations, the Fe(A) ions becomes all crystallograhpically equivalent and we allow their motions in any direction, thus represented by the x, y, and z components of the displacement vector, $u_{{\rm A}x}$, $u_{{\rm A}y}$, and $u_{{\rm A}z}$, respectively (see Fig. 6).

Then the free energy per formula unit of Fe_3O_4, $\mathcal{F}$, can be computed, where there are 4 Fe(A)-O bonds for $\mathcal{E}_{\rm Alat}$ and 12 Fe(B)-O bonds for $\mathcal{E}_{\rm Blat}$, as

$$\mathcal{F} = \mathcal{F}_{\rm BD} + \mathcal{E}_{\rm Alat} + \mathcal{E}_{\rm Blat}, \tag{6}$$

$$\mathcal{F}_{\rm BD} = \alpha(T - T_{\rm c})(u_1^2 + u_2^2), \tag{7}$$

$$\begin{aligned}\mathcal{E}_{\rm Alat} = \frac{K_{\rm A}}{2}\Bigg\{ &\left(\sqrt{u_{{\rm A}x}^2 + \left(\frac{1}{\sqrt{2}} + u_{{\rm A}y} - u_{\rm O1}\right)^2 + \left(\frac{1}{2} + u_{{\rm A}z}\right)^2} - \sqrt{\frac{3}{4}}\right)^2 \\ &+ \left(\sqrt{u_{{\rm A}x}^2 + \left(\frac{1}{\sqrt{2}} - u_{{\rm A}y} + u_{\rm O2}\right)^2 + \left(\frac{1}{2} + u_{{\rm A}z}\right)^2} - \sqrt{\frac{3}{4}}\right)^2 \\ &+ \left(\sqrt{\left(\frac{1}{\sqrt{2}} - u_{{\rm A}x} + u_{\rm O1}\right)^2 + u_{{\rm A}y}^2 + \left(\frac{1}{2} - u_{{\rm A}z}\right)^2} - \sqrt{\frac{3}{4}}\right)^2\end{aligned}$$

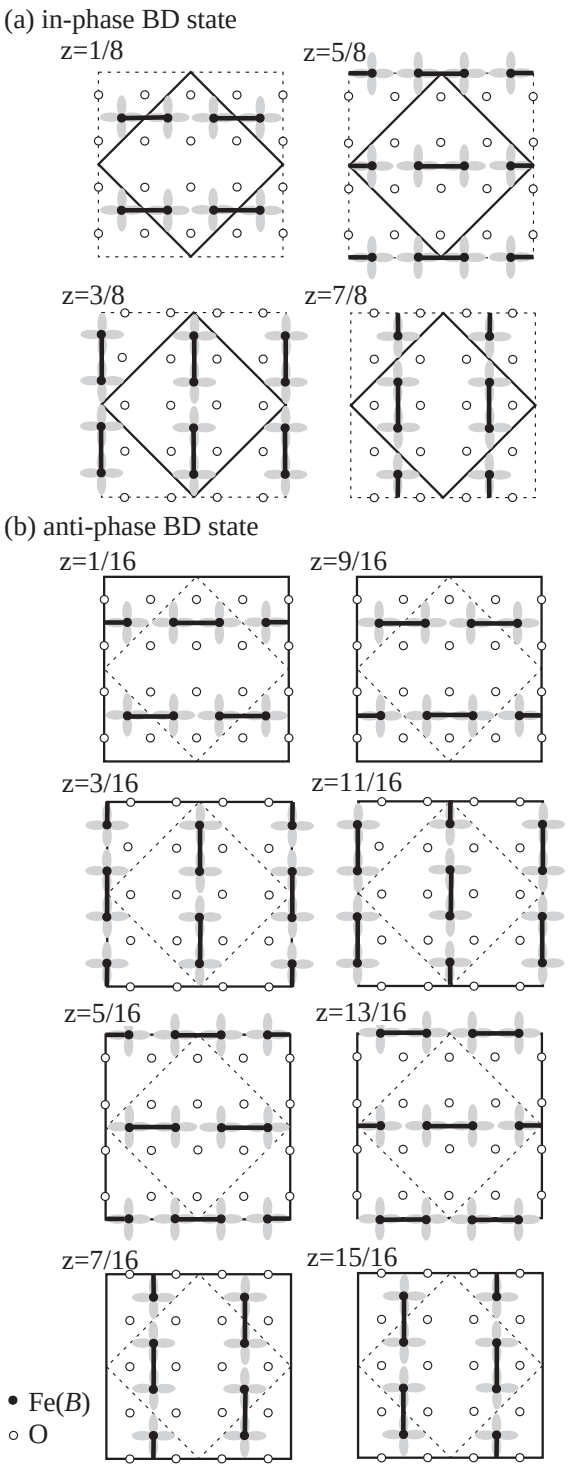

FIG. 5. Schematic representation of (a) the in-phase BD state and (b) the anti-phase BD state both coexisting with the d_{xy}-OO. Only the Fe(B)$_2$O$_4$ layers are shown, where the thick Fe(B)-Fe(B) bonds represent the dimers. The thick squares show the unit cell in the xy plane and the z coordinates indicate the fraction of unit cell size along the z direction. The unit cell remains unchanged from the cubic one above $T_{\rm V}$ shown in Fig. 1 for the in-phase BD pattern, while it becomes $\sqrt{2} \times \sqrt{2} \times 2$ of that for the anti-phase BD pattern.

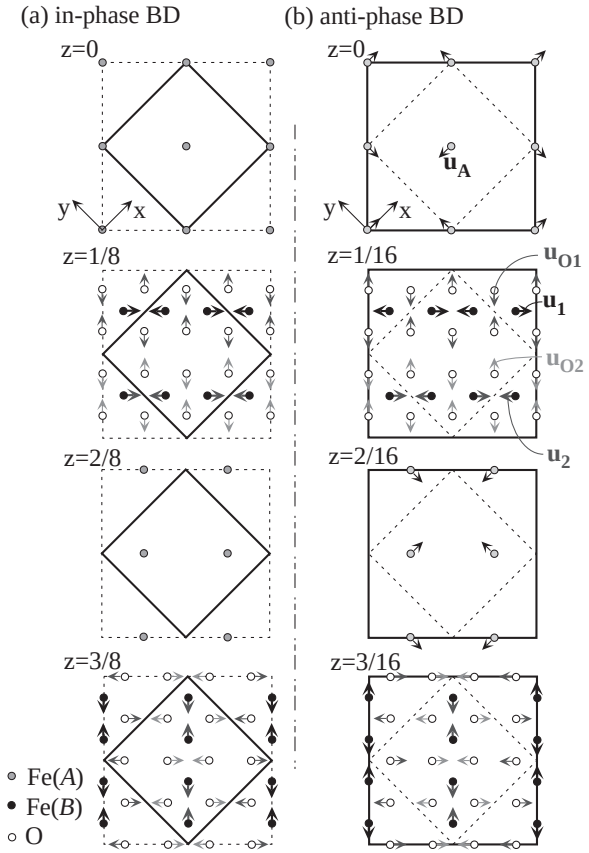

FIG. 6. Schematic representation of the ionic displacements in (a) the in-phase BD pattern and (b) the anti-phase BD pattern. Only two $Fe(B)_2O_3$ and $Fe(A)$ layers each are shown, and the directions of displacement are represented by arrows. The motions of the A sites in (a) is not shown, which are along the z direction.

$$+\left(\sqrt{\left(\frac{1}{\sqrt{2}}+u_{\mathrm{A}x}-u_{\mathrm{O}2}\right)^2+u_{\mathrm{A}y}^2+\left(\frac{1}{2}-u_{\mathrm{A}z}\right)^2}-\sqrt{\frac{3}{4}}\right)^2\Bigg\}, \tag{8}$$

$$\begin{aligned}\mathcal{E}_{\mathrm{Blat}}=\frac{K_{\mathrm{B}}}{2}\Bigg\{&2\left(\sqrt{\left(\frac{1}{\sqrt{2}}-u_1\right)^2+\left(\frac{1}{\sqrt{2}}+u_{\mathrm{O}1}\right)^2}-1\right)^2\\&+2\left(\sqrt{\left(\frac{1}{\sqrt{2}}-u_2\right)^2+\left(\frac{1}{\sqrt{2}}+u_{\mathrm{O}2}\right)^2}-1\right)^2\\&+2\left(\sqrt{\left(\frac{1}{\sqrt{2}}+u_1\right)^2+\left(\frac{1}{\sqrt{2}}-u_{\mathrm{O}1}\right)^2}-1\right)^2\\&+2\left(\sqrt{\left(\frac{1}{\sqrt{2}}+u_2\right)^2+\left(\frac{1}{\sqrt{2}}-u_{\mathrm{O}2}\right)^2}-1\right)^2\\&+\left(\sqrt{1+(u_1-u_{\mathrm{O}1})^2}-1\right)^2+\left(\sqrt{1+(u_2-u_{\mathrm{O}2})^2}-1\right)^2\\&+\left(\sqrt{1+(u_1+u_{\mathrm{O}2})^2}-1\right)^2+\left(\sqrt{1+(u_2+u_{\mathrm{O}1})^2}-1\right)^2\Bigg\},\end{aligned} \tag{9}$$

where the lattice constant of the cubic unit cell is set to 4 so that the length of Fe(A)-O and Fe(B)-O bond without any distortion are 3/4 and 1, respectively. $\mathcal{F}_{\mathrm{BD}}$ describes the instability toward the BD state along each chain as the temperature decreases, discussed in the previous Section.

In Fig. 7, $\mathcal{F}$ as a function of (u_1,u_2) is plotted for the optimized positions of the Fe(A) and O ions, obtained by minimizing it numerically by varying other variables, $u_{\mathrm{A}x}$, $u_{\mathrm{A}y}$, $u_{\mathrm{A}z}$, $u_{\mathrm{O}1}$, and $u_{\mathrm{O}2}$. It is plotted for two sets of elastic constants (a) $K_{\mathrm{A}}=0.1, K_{\mathrm{B}}=0.3$ and (b) $K_{\mathrm{A}}=0.5, K_{\mathrm{B}}=0.3$, at several temperatures. Above T_{c}, the shape of the parabolic curvature gets deeper as T_{c} is approached, almost symmetrically along $u_1=u_2$ and $u_1=-u_2$ suggesting that the fluctuations of both in-phase and anti-phase BD states develop. Below T_{c}, for the parameters in Fig. 7(a), the minimum of the free energy appears along $u_1=u_2$, that is, the in-phase BD state is stabilized, while in Fig. 7(b) the mimimum is along $u_1=-u_2$ which means that the anti-phase BD state is realized. Note that the phase transition is a second order one. The stability of these BD patterns can be understood as follows. In the presence of the in-phase BD pattern, all the Fe(B)$_4$O$_4$ cubes [25], connecting the Fe(B)$_2$O$_4$ xy planes show ionic displacements as shown in Fig. 8(a), where all the interlayer Fe(B)-O pairs move respectively in the same direction, providing small $\Delta u_{\mathrm{B-O}}$'s. Thus the lattice elastic energy of the Fe(B)-O bonds, $\mathcal{E}_{\mathrm{Blat}}$, should be the lowest for the in-phase BD states with such configuration, compared to other BD patterns containing cubes as shown in Figs. 8(b) and 8(c), with both Fe(B) pairs forming dimers or both being inter-dimer Fe(B) pairs, respectively. For example, the anti-phase BD shows all of these three kinds of cubes, realized with the ratio of $2:1:1$, in order, thus costing rather higher $\mathcal{E}_{\mathrm{Blat}}$ than in-phase BD. On the other hand, the Fe(A)-O tetrahedra would be quite deformed in the presence

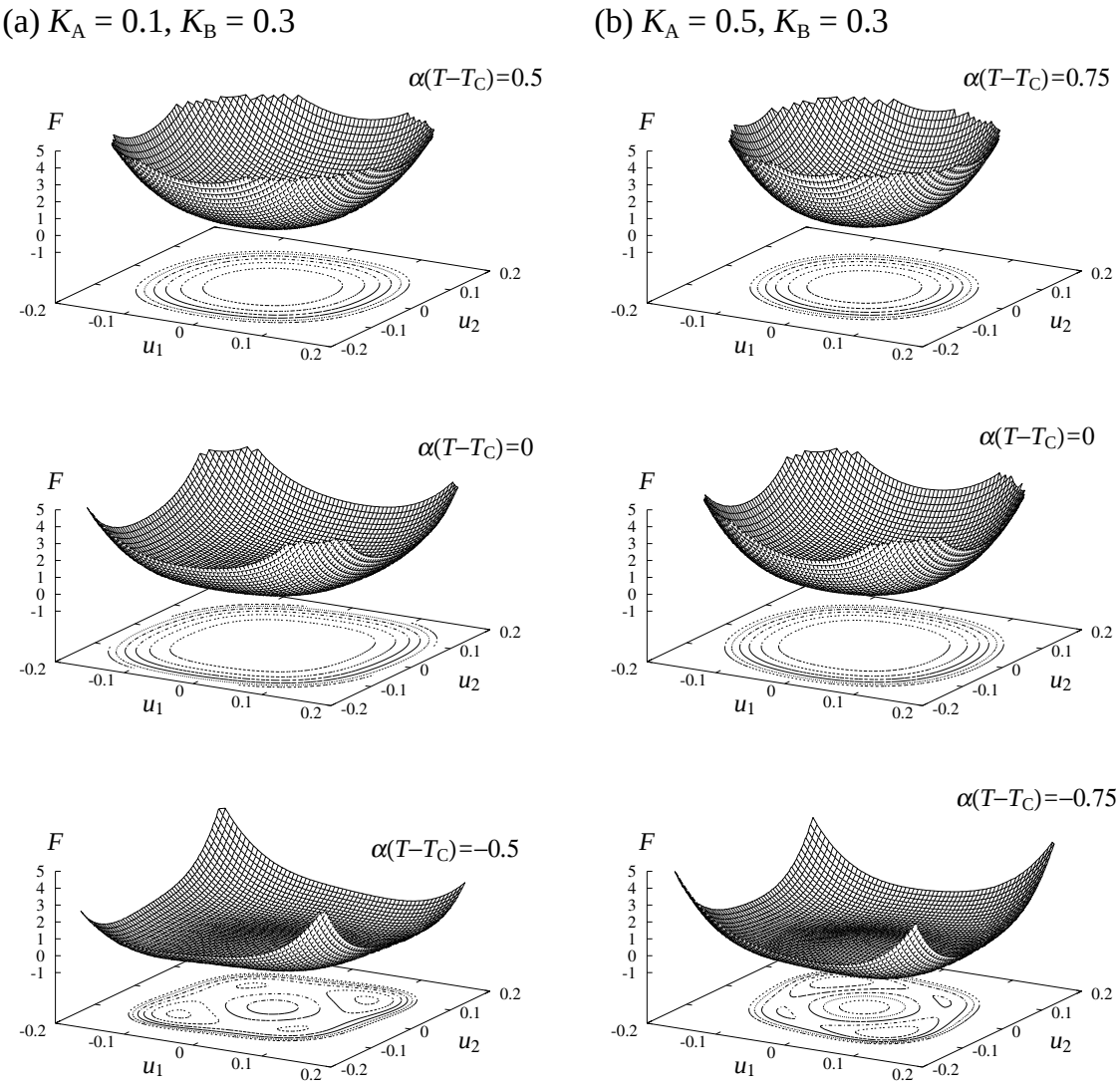

FIG. 7. Calculated free energy, $\mathcal{F}$, for (a) $K_A = 0.1, K_B = 0.3$ and (b) $K_A = 0.5, K_B = 0.3$ at several temperatures, as a function of the degree of dimerization for adjacent chains, (u_1, u_2). Note that the contour plot in the base is guide for eyes.

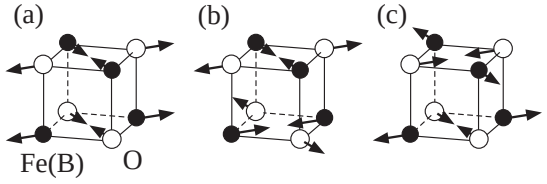

FIG. 8. Schematic view of the lattice displacements in the Fe(B)-O cubes connecting adjacent Fe(B)$_2$O$_4$ layers when the BD state is stabilized. In the in-phase BD pattern only the displacement pattern (a) is realized, while in the anti-phase BD pattern (a), (b) and (c) are realized with the ratio of 2 : 1 : 1.

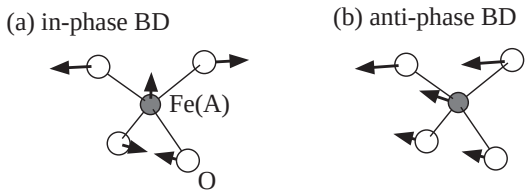

FIG. 9. Schematic view of the displacements in the Fe(A)-O tetrahedra for (a) the in-phase BD pattern and (b) the anti-phase BD pattern.

of the in-phase BD, which is shown in Fig. 9(a), providing large lattice elastic energy of the Fe(A)-O bonds, $\mathcal{E}_{\rm Alat}$, while the anti-phase BD pattern make the O ions surrounding the Fe(A) ions showing displacements as shown in Fig. 9(b), where the cost in $\mathcal{E}_{\rm Alat}$ will be rather smaller. This is because the motion of the oxygens are in the same direction for the latter pattern so that the Fe(A) ions can adjust their position to lower $\Delta u_{\rm A-O}$, as can be seen in Fig. 9(b). To summarize, one can say that $\mathcal{E}_{\rm Blat}$ favors the in-phase BD state while $\mathcal{E}_{\rm Alat}$ favors the anti-phase one.

These naive discussions are consistent with the above calculation of the Landau-type free energy. There, we have observed that a competition arises between the in-phase and anti-phase BD states, stabilized for $K_{\rm A} \lesssim K_{\rm B}$ and for $K_{\rm A} \gtrsim K_{\rm B}$, respectively. We propose that the latter is the case in magnetite, since in general, large deformation is hardly realized in the tetrahedra of oxygen surrounding the A sites of the spinel structure, which may be due to its tight packing compared to the B sites [26]. The importance of such ionic displacement of the O ions surrounding the A sites in determining the electronic properties in the ground state has recently also been pointed out in another spinel compound AlV_2O_4 [27]. This anti-phase BD state provides the correct unit cell determined experimentally [28], as will be discussed later.

IV. COMPARISON WITH EXPERIMENTS

Based on the discussions above, our proposal for the physical properties in magnetite Fe_3O_4 can be summarized in Fig. 10, which has the following new features: the existence of OO in the B sites at all temperature range below room temperature, the BD fluctuation (both the in-phase and the anti-phase BD's) above the Verway transition temperarure, $T_{\rm V}$, and the anti-phase BD stabilized in the insulating phase as a consequence of compensation with the lattice elastic energy of the whole system. These are compared with the known experimental facts in the following.

Below the Verway transition temperature, the existence of ferro-OO is supported with dielectric measurements showing large anisotropy [29]. Above $T_{\rm V}$, in contrast, crystal structure analysises show no evidence of the lowered symmetry from the cubic one, apparently contradicting with our prediction of the ferro-OO even in the metallic phase. However, the symmetry in the electronic structure has been pointed out to be lowered than the cubic one [30] based on magneto-crystalline anisotropy measurements [31] and in the recent resonant X-ray scattering at room temperature [13], consistent with the OO state.

As for the BD, there is a strong support from neutron scattering measurement by Shapiro *et al.* [32], which is the observation of *1D correlation* above $T_{\rm V}$, not explained

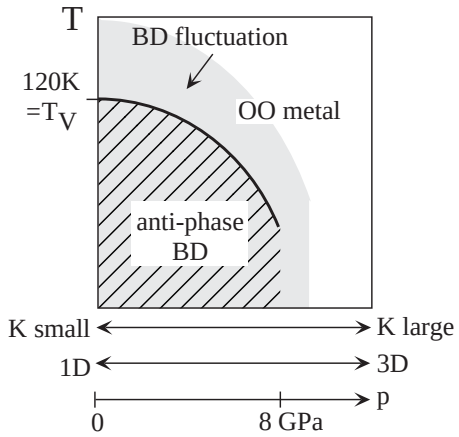

FIG. 10. Schematic phase diagram for magnetite Fe_3O_4. The OO and BD denotes the orbital-ordered and bond dimerized states, respectively. The vertical axis is the temperature, T, while the horizontal axis can be interpreted either as the pressure, p, the "rigidness" of the lattice represented by the lattice constant, K, or the effective dimensionality. The bold line is the Verway transition temperature, $T_{\rm V}$, varying as a function of such parameters.

by the CO but consistent with the present BD picture. This 1D nature of the BD transition can naturally provide an explanation for the critical fluctuation above $T_{\rm V}$ observed in large temperature range up to room temperature, such as in the pseudogap structure of the optical conductivity [33] and in neutron scattering measurements where it has actually been realized that the atomic displacement is playing an important role [12]. Moreover, our scenario that the Verway transition is a phase transition from OO metal to the coexistent state of OO and BD explains the entropy change of $\Delta S = R\log 2$ per mole of Fe_3O_4 estimated from specific heat measurements [34], arising from the degree of freedom for dimerization. This excludes the order-disorder-type CO picture of Verway [3] predicting $\Delta S = 2R\log 2$ as well as simultaneous OO and BD transition with $\Delta S = 2R\log 3$ from the orbital degree of freedom.

The crystal structure in the presence of anti-phase BD provides the correct unit cell size below $T_{\rm V}$ in the actual compound, namely, $\sqrt{2}\times\sqrt{2}\times 2$ of the cubic unit cell above $T_{\rm V}$ shown in Fig. 1 [28], which is also supported by the double period modulation along the z axis observed in electron diffraction [35] and in neutron scattering [36]. Furthermore, the diffusive spot above $T_{\rm V}$ of the corresponding wave vector $(0,0,1/2)$, observed in a neutron scattering measurement showing a divergent behavior toward $T_{\rm V}$ [12] can be assigned to the anti-phase BD fluctuation developping above $T_{\rm V}$ seen in the calculation of Sec. III. On the other hand, the analysis of Yamada *et al.* [37] of their neutron scattering data above $T_{\rm V}$ apparently seems to correspond to the in-phase one, where the ionic motions of the Fe(B)-O cubes are proposed to be as in Fig. 8(a). This might be the observation of the fluctuation of the in-phase BD mode, which is also seen in our calculation though a long range order of this mode is not achieved. We have seen that such competition arises due to the existence of two kinds of elastic energies, $\mathcal{E}_{\rm Alat}$ and $\mathcal{E}_{\rm Blat}$, which may be consistent with the experimental findings by Shapiro *et al.* that "two types of interacting dynamical variables are taking part in the neutron scattering" [32].

The observed pressure induced metallic behavior [16] can be naturally understood since

the pressure should effectively increase the value of K in Eq. (3) (or $K_{\rm A}$ and $K_{\rm B}$ in Eqs. (4) and (5)) making the lattice more "rigid", and/or increase the three-dimensionality of the system, both expected to destabilize the BD state, which is represented in Fig. 10. This is analogous to the case of spin-Peierls transition, the mapped state of the BD state as mentioned in Sec. II B, known to be destroyed by enhancement in the electron-lattice coupling constant and/or the three-dimensionality [38]. We point out the possibility that the three-dimensional BD pattern may be changed under different environments such as pressure and temperature, since there are two competing phases, the in-phase and the anti-phase BD states, as seen in Sec. III. Search for such transition between these phases under uniaxial pressure is also interesting, since these states are highly anisotropic. Another possibility is that incommensurate phases may be stabilized as a consequence of such competition, as observed in dielectrics $[{\rm N}({\rm CH}_3)_4]_2M{\rm Cl}_4$ [39] as well as in CO systems such as perovskite Ni oxides [40] and NaV_2O_5 [41], due to competing different states.

One discrepancy between our theory and the experimental facts is the order of the phase transition: experimentally it is first order while it is second order in our calculations in Secs. II and III. This discrepancy may be due to the simplified approximation we made for the strucural change as discussed in Sec. III. In the actual compound, the lattice distortion will be more complicated than in our calculation, represented as in Fig. 6, e.g., the lattice distortion of the B sites along the chain should take the period of four sites which is contained in the unit cell, as $(u_a, -u_b, u_c, -u_d, u_a, -u_b, ...)$, rather than $(u, -u, u, -u, ...)$ as in our calculation. This should make the crystal symmetry of the BD insulating phase lower than that in our calculation, which may lead to a first order phase transition [42].

Finally, it is noted that the recent findings of possible charge disproportionation in the B sites by X-ray anomalous scattering [43] does not contradict with our proposal here. The anti-phase BD state gives rise to crystallographically independent Fe(B) ions, which should make the charge density on the B sites different where the amount of charge disproportionation will be not so large but can be detectable in a sensitive probe such as X-ray anomalous scattering measurements.

V. CONCLUSION

In conclusion, we have theoretically proposed a new model for the mechanism of the Verway transition in magnetite Fe_3O_4. It is not a charge ordering transition as has been believed for more than a half century, but a bond dimerization induced by the Peierls instability in a one-dimensional state as a consequence of the ferro-orbital ordering due to strong electronic correlation. The actual bond dimerization pattern is predicted to be the anti-phase one, based on discussions on the lattice elastic energy of the system. This model seems to be able to provide the explanation for the long lasting mystery of the Verway transition in this compound.

ACKNOWLEDGMENTS

We thank Y. Fujii, T. Katsufuji, N. Môri, N. Nagaosa, Y. Nakao, K. Ohwada, H. Takagi and S. Todo for valuable discussions and suggestions. We also thank T. Katsufuji and T. Toyoda for providing us Refs. 27 and 43, respectively, and A. Himeda and T. Koretune for technical supports on numerical calculations. This work is supported by the Grant-in-Aid from Ministry of Education, Science, Sports and Culture of Japan.

REFERENCES

[1] for recent reviews, M. Imada, A. Fujimori, and Y. Tokura, Rev. Mod. Phys. **70**, 1039 (1998), Sec. E.1; N. Tsuda, K. Nasu, A. Fujimori, and K. Shiratori, *Electronic Conduction in Oxides*, 2nd ed. (Springer-Verlag, Berlin, 2000), p. 243.

[2] E. J. W. Verway, Nature (London) **144**, 327 (1939).

[3] E. J. W. Verway and P. W. Haayman, Physica **8**, 979 (1941); E. J. W. Verway, P. W. Haayman, and F. C. Romeijn, J. Chem. Phys. **15**, 181 (1947).

[4] J. R. Cullen and E. R. Callen, Phys. Rev. B **7**, (1973) 397

[5] D. Ihle and B. Lorenz, Phil. Mag. B **42**, 337 (1980).

[6] A. Yanase and K. Shiratori, J. Phys. Soc. Jpn. **53**, 312 (1984).

[7] Z. Zhang and S. Satpathy, Phys. Rev. B **44**, 13319 (1991).

[8] V. I. Anisimov, I. S. Elfimov, N. Hamada, and K. Terakura: Phys. Rev. B **54** (1996) 4387.

[9] M. Mizoguchi, J. Phys. Soc. Jpn. **44**, 1512 (1978).

[10] J. M. Zuo J. C. H. Spence, and W. Petuskey, Phys. Rev. B **42**, 8451 (1990).

[11] P. W. Anderson, Phys. Rev. **102**, 1008 (1956).

[12] Y. Fujii, G. Shirane, and Y. Yamada, Phys. Rev. B **11**, 2036 (1975).

[13] J. García, G. Subías, M. G. Proietti, H. Renevier, Y. Joly, J. L. Hodeau, J. Blasco, M. C. Sánchez, and J. F. Bérar: Phys. Rev. Lett. **85**, 578 (2000).

[14] P. Novak, H. Stepankova, J. Englich, J. Kohout, and V. A. M. Brabers: Phys. Rev. B **61**, 1256 (2000).

[15] J. García, G. Subías, M. G. Proietti, J. Blasco, H. Renevier, J. L. Hodeau, and Y. Joly: Phys. Rev. B **63**, 054110 (2000).

[16] S. Todo, N. Takeshita, T. Kanehara, T. Mori, and N. Môri, J. Appl. Phys. **89**, 7347 (2001).

[17] for reviews, H. Fukuyama, H. Seo, and H. Kino, Physica B **280**, 462 (2000); H. Fukuyama and H. Seo, J. Phys. Soc. Jpn. **69** Suppl. B, 144 (2000).

[18] H. Kino and H. Fukuyama, J. Phys. Soc. Jpn. **65**, 2158 (1996); K. Kanoda, Hyperfine Int. **104**, 235 (1997).

[19] J. Bernasconi, M. J. Rice, W. R. Schneider, and S. Strässler, Phys. Rev. B **12**, 1090 (1975).

[20] K. Mishra, Z. Zhang, and S. Satpathy, J. Appl. Phys. **76**, 15 (1994).

[21] The t_{2g}-orbital level in the spinel structure splits into e_g and a_{1g} symmetry combinations, though, band structure calculation shows that the octohedral component in the crystal field at the B site in Fe_3O_4 is so strong that the splitting is negligible [7].

[22] J. C. Slater and G. F. Koster, Phys. Rev. **93**, 1498 (1954); W. A. Harrison, *Electronic Structure and the Properties of Solids* (Dover, New York, 1989).

[23] We have repeated the calculation of Mishra *et al.* [20] and the value we obtained for V_c was 0.29 eV, smaller than theirs. The difference should be due to the larger number of mesh in our calculation taken for the k-integration, though it is not important for the discussion here.

[24] H. Seo and M. Ogata, Phys. Rev. B **64**, 113103 (2001).

[25] Strictly saying, the Fe(B)-O network is formed not in cubes but in parallelepipeds, though it is approximately cubes so the we call them so in this paper for simplicity.

[26] E. J. W. Verway and E. L. Heilmann, J. Chem. Phys. **15**, 174 (1947).
[27] K. Matsuno, T. Katsufuji, S. Mori, Y. Moritomo, A. Machida, E. Nishibori, M. Takata, M. Sakata, N. Yamamoto, and H. Takagi, J. Phys. Soc. Jpn **70**, 1456 (2001).
[28] M. Iizumi, T. F. Koetzle, G. Shirane, S. Chikazumi, M. Matsui, and S. Todo, Acta Cryst. **38**, 2121 (1982).
[29] M. Kobayashi, Y. Akishige, and E. Sawaguchi, J. Phys. Soc. Jpn. **55**, 4044 (1986).
[30] K. Siratori and Y. Kino, J. Magn. Magn. Mat. **20**, 87 (1980).
[31] K. Abe, Y. Miyamoto, and S. Chikazumi: J. Phys. Soc. Jpn. **41**, 1894 (1976).
[32] S. M. Shapiro, M. Iizumi, and G. Shirane, Phys. Rev. B **14**, 200 (1976).
[33] S. K. Park, T. Ishikawa, and Y. Tokura, Phys. Rev. B **58**, 3717 (1998).
[34] J. P. Shepherd, J. W. Koenitzer, R. Aragón, C. J. Sandberg, and J. M. Honig: Phys. Rev. B **31**, 1107 (1985).
[35] T. Yamada, K. Suzuki, and S. Chikazumi, Appl. Phys. Lett. **13**, 172 (1968).
[36] E. J. Samuelson, E. J. Bleeker, L. Dobrzynski, and T. Riste, J. Appl. Phys. **39**, 1114 (1968); G. Shirane, S. Chikazumi, J. Akimitsu, K. Chiba, M. Matsui, and Y. Fujii, J. Phys. Soc. Jpn. **39**, 949 (1975).
[37] Y. Yamada, M. Mori, Y. Noda, and M. Iizumi, Solid State Comm. **32**, 827 (1979); Y. Yamada, N. Wakabayashi, and R. M. Nicklow, Phys. Rev. B **21**, 4642 (1980).
[38] H. Fukuyama and S. Inagaki: in *Magnetic properties of Low-Dimensional Systems*, edited by L. M. Falikov and J. L. Morán-López (Springer-Verlag, 1986), p. 156.
[39] S. Shimomura, N. Hamaya, and Y. Fujii, Phys. Rev. B **53**, 8975 (1995).
[40] P. Wochner, J. M. Tranquada, D. J. Bettrey, and V. Sachan, Phys. Rev. B **57**, 1066 (1998); H. Yoshizawa, T. Kakeshita, R. Kajimoto, T. Tanabe, T. Katsufuji, and Y. Tokura, *ibid.* **61**, 854 (2000).
[41] K. Ohwada, H. Nakao, H. Nakatogawa, N. Takesue, Y. Fujii, M. Isobe, Y. Ueda, Y. Wakabayashi, and Y. Murakami, J. Phys. Soc. Jpn. **69**, 639 (2000); K. Ohwada, Y. Fujii, N. Takesue, M. Isobe, Y. Ueda, H. Nakao, Y. Wakabayashi, Y. Murakami, K. Ito, Y. Amemiya, H. Fujihisa, K. Aoki, T. Shobu, Y. Noda, and N. Ikeda, Phys. Rev. Lett. **87**, 086402 (2001).
[42] L. D. Landau and E. M. Lifshitz, *Statistical Physics* (Addison-Wesley, Reading, Massachusetts, 1958) Chap. XIV.
[43] T. Toyoda, S. Sasaki, and M. Tanaka, Jpn. J. Appl. Phys. **36**, 2247 (1997); Am. Miner. **84**, 284 (1999).